ARTICLE TEMPLATE

Classification of the mechanism of toxicity as applied to human cell line ECV304

Yasser Abd Djawad[a], Janice Kiely[b] and Richard Luxton[b]

[a]Department of Electronics, Universitas Negeri Makassar, Makassar, Indonesia; [b]Institute of Biosensing Technology, Bristol, UK

ARTICLE HISTORY
Compiled October 29, 2020

ABSTRACT
The objective of this study was to identify the pattern of cytotoxicity testing of the human cell line ECV304 using three techniques of an ensemble learning algorithm (bagging, boosting and stacking). The study of cell morphology of ECV304 cell line was conducted using impedimetric measurement. Three types of toxins were applied to the ECV304 cell line namely 1 mM hydrogen peroxide (H_2O_2), 5% dimethyl sulfoxide (DMSO) and 10 μg Saponin. The measurement was conducted using electrodes and lock-in amplifier to detect impedance changes during cytotoxicity testing within a frequency range 200 and 830 kHz. The results were analysed, processed and extracted using Detrended Fluctuation Analysis (DFA) to obtain characteristics and features of the cells when exposed to the each of the toxins. Three ensemble algorithms applied showed slightly different results on the performance for classifying the data set from the feature extraction that was performed. However, the results show that the cell reaction to the toxins could be classified.

KEYWORDS
cell morphology, impedance, machine learning.

1. Introduction

The results of measurements or experiments in biological and medical research generally produce complex data sets, both in terms of size and dimensions (Zitnik et al. 2019). In addition, the resulting data sets experience a bias and error from the measurement process as well as from the nature of the biological entity being studied (Kihm et al. 2018; William et al. 2019). This problem raises new opportunities for data processing using an algorithmic approach rather than the usual statistical methods (Wang 2006; Zhao et al. 2019). The algorithm must provide information on the differences, categories and treatments associated with the measurement data sets.

Machine learning is part of Artificial Intelligence (AI) which has the ability to learn automatically by analysing data and improve their learning from experience to perform certain tasks without being explicitly programmed (Bishop 2006). This learning process utilise a special algorithm known as the machine learning algorithm. Machine learning algorithms create a model based on the data provided and make predictions or decision based on that model. A good classification model is able to

CONTACT Y.A.Djawad. Email: yasser.djawad@unm.ac.id

separate data based on its class. The ability of machine learning to create a model from data and to separate different patterns into groups makes this technique of common use by biological researchers (Sommer and Gerlich 2013). Machine learning is commonly used in classification (Vlahou et al. 2003). In the classification process, the user provides a training data set collected from the experiment as an input with predefined classes or labels associated with each type of data in the set. This training data set is used by the machine learning algorithm to determine the pattern of the data. Once the pattern or model is defined then the test data can be applied for prediction. This type of machine learning is well known as supervised machine learning. A considerable amount of literature has been published on the use of machine learning to analyse biological and medical data, such as for classifying red blood cells (Aliyu et al. 2018; Tiwari et al. 2018; Nassar et al. 2019), antibiotic (Yang et al. 2019), cell images (Meng et al. 2018; Forslöw 2018; Oei et al. 2019; Iqbal et al. 2019; Gu et al. 2019), cells (Chen and Chefd'hotel 2014; Xia et al. 2018; Singh et al. 2018; Lam et al. 2019; Ozaki et al. 2019), and it has been used widely in drug discovery (Liu et al. 2019; Yin et al. 2019; Ekins et al. 2019), study of cancer (Rachman and Rustam 2016; Rubin et al. 2019) and study of disease (Pan et al. 2018).

Moreover, new techniques and algorithms have been developed to improve the results of machine learning. One of these techniques is ensemble classification. Ensemble classification combines several classifiers to provide better prediction of the overall performance compared to a single classifier. Three techniques of ensemble classification are bagging (Breiman 1996), boosting (Schapire 1990) and stacking (Wolpert 1992). Ensemble classification has been used in the study of cancer by researchers (Hijazi et al. 2012; Tarek et al. 2016; Cong et al. 2017) to yield improved performance in terms of the output variables of machine learning, such as increased accuracy and reduced errors. However, there are many feature selection methods and the classifier can be used in ensemble learning and it is not possible to use all of them to get ensemble learning results or prediction since the group of classifiers have to be chosen (Park and Cho 2003; Hijazi and Chan 2013).

The morphology of cells change depending on the type of toxin applied. To see the different types of changes from the given toxins, feature extraction and machine learning algorithm are required to classify the data based on the type of toxin. Feature extraction is a process used to reduce the dimensions of large raw data set, so that it can be managed and processed to reduce the computing process without reducing the characteristics of the raw data. In this study, three techniques of ensemble learning (bagging, boosting and stacking) were applied to the results of cytotoxicity test on cell line ECV304 using various toxins, i.e hydrogen peroxide (H_2O_2), dymethil sulfoxide (DMSO) and Saponin. ECV304 cell line was chosen since ECV304 cell line exhibits many endothelial features given the dearth of suitable endothelial cell lines, make it an attractive in vitro model for endothelial (Suda et al. 2001). Meanwhile, the toxins were selected as they were readily available, they are not highly hazardous and they have well defined effects on cells. The toxins and their concentration were applied dependent on their physical properties and mechanism of toxicity. Applied toxins were: H_2O_2, a powerful oxidizing operator; DMSO, a strong cell separating agent; and saponin, an intense layer permeabilizing agent. Both H_2O_2 and DMSO have similar, significant effects on the cells related to both morphology and metabolism of cells, whereas saponin forms pores in the cell membrane through which fluid is drawn into the cell due to osmotic pressure. The use of this range of toxins allowed assessment of the ability of the technique to differentiate between both closely related toxins and those which display dissimilar modes of action. Therefore, the aim of this study was to

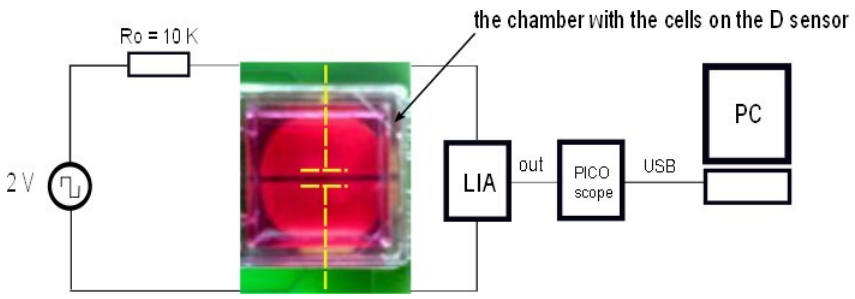

Figure 1. Circuit of the experiment

prove that the mechanism of toxicity as when given to ECV304 cells could be classified.

2. Materials and methods

2.1. Cells preparation

ECV304 cells from the European Collection of Cell Cultures were seeded in a 75 cm^2 flask in complemented 12 mL M199 media (Gibco) supplemented with 10% foetal calf serum and 2 mL L-glutamine at a density of $3x10^5$ cells/mL and maintained in a humidified incubator at 37°C with 5% CO_2. The cells were routinely fed with fresh medium every 3 days and monitored daily by microscope to check for confluence, at which point the cell monolayer covers 75-80% of the surface of the flask. Once confluence was reached, the cell layer was rinsed with Phosphate Buffered Saline (PBS) followed by 1 mL of Trypsin-EDTA solution (0.05% porcine trypsin, 0.2 g/L EDTA) followed by incubation at 37 °C for approximately 5 minutes to allow the cells to detach from the flask surface. The trypsin was deactivated when the cells had detached, by the addition of 2 mL of growth medium and the cell density counted by the Trypan Blue Exclusion method. The cell suspension was diluted to a density of $3x10^5$ cells/mL and 2 mL of cell suspension added to a LAB-TEK chamber and maintained at 37 °C and 5% CO_2. From the cell suspension, the cells were separate in a 2 mL chamber as a control which the cells were not given any toxins. Cytotoxicity testing was performed by adding 1 mM H_2O_2, 5% DMSO or 10 μg Saponin. This experiment was repeated 20 times for each exposed toxin to obtain classification data and the classification only relates to the specific toxins that have been examined.

2.2. Instrumentation

In this study, Impedance spectroscopy (IS) was used. IS is a measurement technique for investigating the electrical properties of a material using electrically conducting electrodes (Barsoukov and Macdonald 2005). IS has been applied in many biological research studies for instance for monitoring cell cycle of Human cervical carcinoma cells (HeLa) (Wang et al. 2010), to perform a cytotoxicity testing on BALB/3T3 A-31-1-1 cell line using sodium arsenite, cadmium chloride and cis-platinum (Ceriotti et al. 2007) and to monitor changes of porcine brain capillary endothelial cells (PBCECs) shape during apoptosis (Arndt et al. 2004). The impedance measurements used a lock-in amplifier (LIA) (Sengupta et al. 2005) connected to D patterned sensor as depicted

in Figure 1. PCB fabrication technique was applied to the D patterned sensor. The D patterned sensor composed a copper layer coated with 0.1 μm gold over 5 μm nickel. The diameter of each sensor was 22 mm, with 1 mm space between the counter and detecting electrodes to correspond to the surface of the cell chamber. A 10 KΩ resistor was connected in series with the D patterned sensor to limit the current and to achieve a large bandwidth for the RC circuit. The LIA was connected in parallel with the sensors. The chamber (Nunc LAB-TEK II Chambered Coverglass, USA) was placed on the D sensor such that the cells were not in direct contact with the sensor to avoid cross-contamination with the previous experiment and facilitating multiple, sequential measurement a single sensor pair. The chamber base is made of borosilicate coverglass with thickness 0.13-0.16 mm and the culture area was 4.2 cm^2. In order to ensure that the electric field penetrated the cell culture, a thin coverglass was used. During the experiments, the D sensor and the cell chamber were placed in the incubator. A 2 V square wave signal was used as an input, and the measurement of voltage output from the LIA were provided by a real-time PC-Based oscilloscope (PICOscope-Pico Technology, UK), which was controlled and monitored from a PC. Data were acquired for each data set at 1, 80 and 120 minutes after either H_2O_2, DMSO or Saponin had been added. The total data set from each experiment comprised of 64 blocks; sampled from 200 kHz to 830 kHz with an interval 10 kHz. A broadband approach to impedance measurement can be used to investigate multiple cell properties. In a model, developed by (Ren and Chui 2018), for a single cell, cell interactions were classified into 3 frequency bands; 0.1 – 10 KHz, 10 kHz – 1 MHz, 1MHz to 10MHz. The high frequency band was associated with changes in the cytoplasm of the cell, while changes in the cell membrane were generally associated with mid frequency bands. Lower frequency signals did not penetrate the cells. Finally, it was suggested that cell size could be associated with all frequency bands in their model, as there is clearly interdependency in the changes in size with both changes on cytoplasm and cell membrane. The mid-frequency band was selected for this study as it most effectively encompassed the morphological changes in the cells. The power of the technique presented here is that the whole of the mid-range can be evaluated from the impedance spectra, so both specific and broad acting toxins can be identified through the technique.

2.3. Feature extraction

The measurement result produced 64 values for each toxin. Detrended Fluctuation Analysis (DFA) was applied to the output signal to obtain features of the signals. Detrended Fluctuation Analysis (DFA) is a statistical technique for scaling long range correlations in a time series (Peng et al. 1995). The time series is divided into several windows (or scales) with width n as shown in Figure 2. Three scales (6, 12 and 24) were applied to the output signals. the average fluctuation $F(n)$ of the signal is computed as follows :

$$F(n) = \sqrt{\frac{1}{N}\sum_{k=1}^{N}(y(k) - y_n(k))^2} \quad (1)$$

Hurst exponent (α) is defined as the slope of data trend in the F(n) graph. The average fluctuation (Fn) and Hurst exponent (α) of the output signals were performed at 1, 80 and 120 minutes of measurements for each scale as shown in Figure 3 and

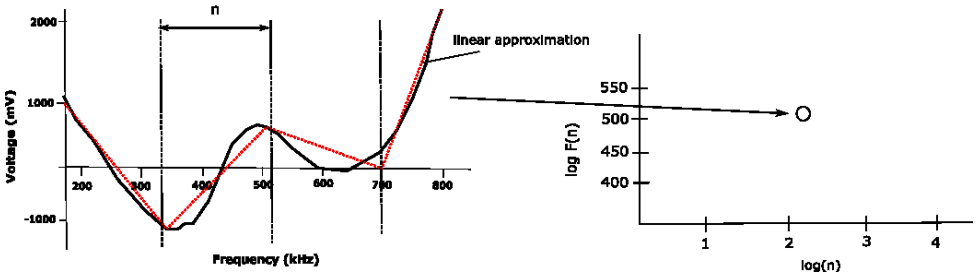

Figure 2. The DFA method for a width of window (n). Similar method repeats for various width of windows

4 (Djawad et al. 2019). There were 20 experiment for each toxin tested. This means that 60 experiments for the 3 toxins were conducted. In total, there were 80 samples gathered from the experiment including control cells for 20 samples. Each experiment provided 1 sample. There were 6 features for each sample were gathered from the average fluctuation (Fn) and Hurst exponent (α) of the signals at 1, 80 and 120 minutes. The class distribution was balanced since each cytotoxicity testing has 20 samples including control cells as well had 20 samples.

2.4. Ensemble machine learning

Three ensemble techniques were applied for analysing the data; bootstrap aggregating (bagging), boosting and stacking. Bagging consists of two processes namely bootstrap and aggregation. Bootstrap is a statistical technique for retrieving data by sampling using a random process with replacement to generate multiple sets of training data. While aggregation is a process of collecting all the results with similar classifier output for each bootstrap samples for final combined prediction decision as shown in Figure 5a. One of the methods using bagging algorithms is Random Forest (RF). Boosting is a sequential tree process using information from the previous classifier output. Prediction at each stage is based on the output of the previous classifier results. This process learns from previous predictions to improvise the final decision as shown in Figure 5b. In this study the gradient boosting machine (*gbm*) method was applied. Stacking is an ensemble learning technique that combines several different classifier results (multi classifier) using the same initial data set. Each classifier produces an output that will be used as data for the meta classifier for the final combined decision, as shown in Figure 5c. In this study, Logistic regression classifier (LR), Linear Discriminant Analysis (LDA), k-nearest Neighbors, (k-NN), Support Vector Machine (SVM), Decision Tree and Naive Bayes were used as classifiers and the RF was used as the meta classifier.

2.4.1. Cross-Validation

Cross-Validation (CV) is a resampling technique used to assess machine learning models on a constrained data set. The technique splits the data set into k groups or folds. Generally, there are 3 techniques used; k-fold CV, stratified k-fold CV and Leave One Out Cross Validation (LOOCV). k-fold CV involves dividing given data into a number of k folds where each fold is used as a test set in the end. For instance the situation of 4-fold cross validation (k = 4), where the data is divided into 4 folds is shown in Figure 6a. In the first round, the first fold is used to test the model and the rests are used to train the model. In the next cycle, the second fold is used as a

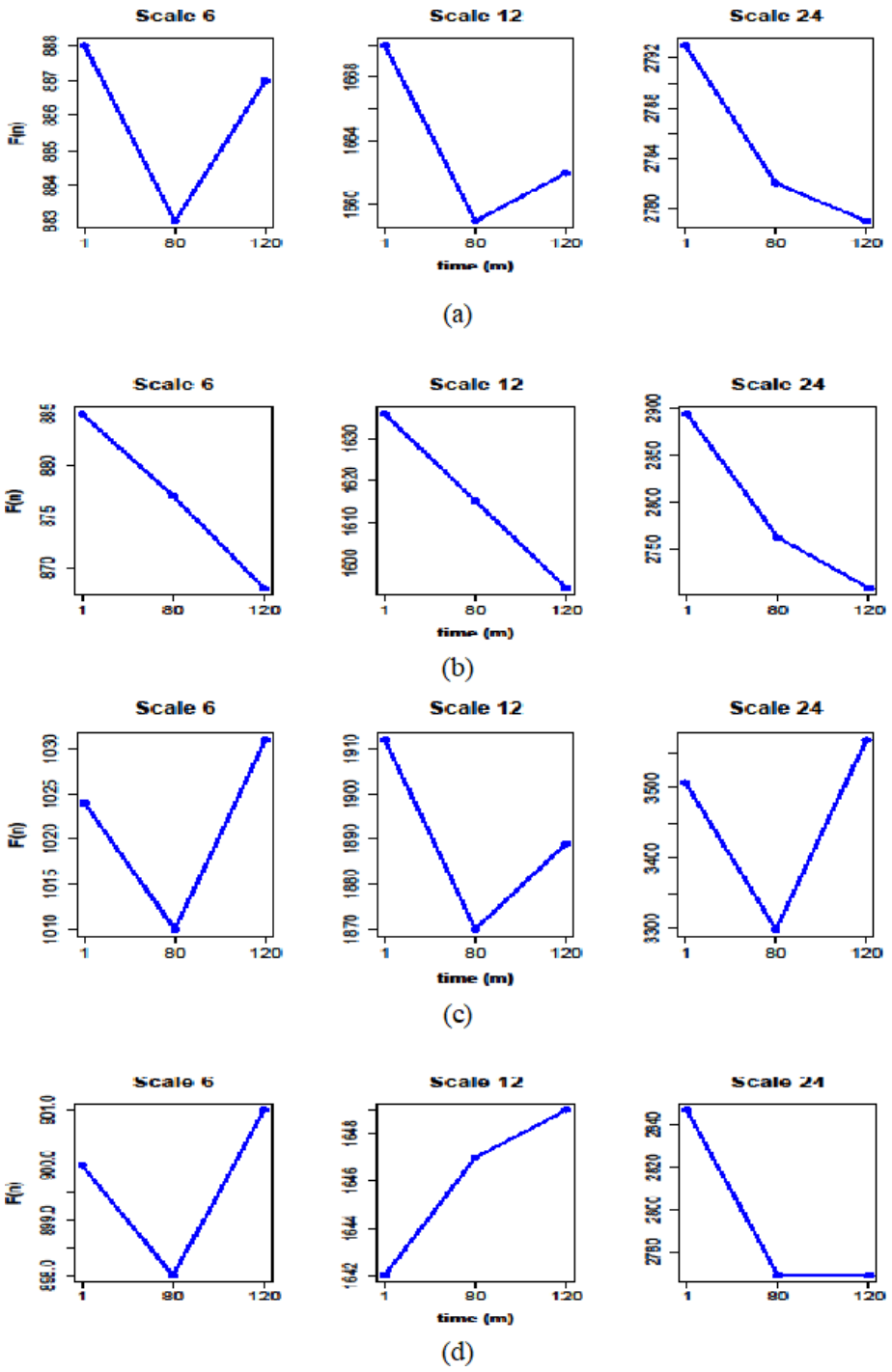

Figure 3. The average fluctuation F(n) of (a) Control cells (b) cells + H_2O_2 (c) cells + DMSO (d) cells + saponin.

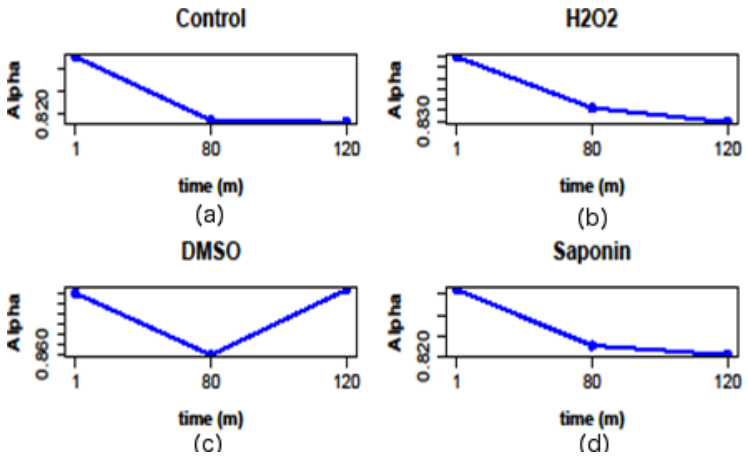

Figure 4. The Hurst exponent (α) of (a) Control cells (b) cells + H_2O_2 (c) cells + DMSO (d) cells + saponin.

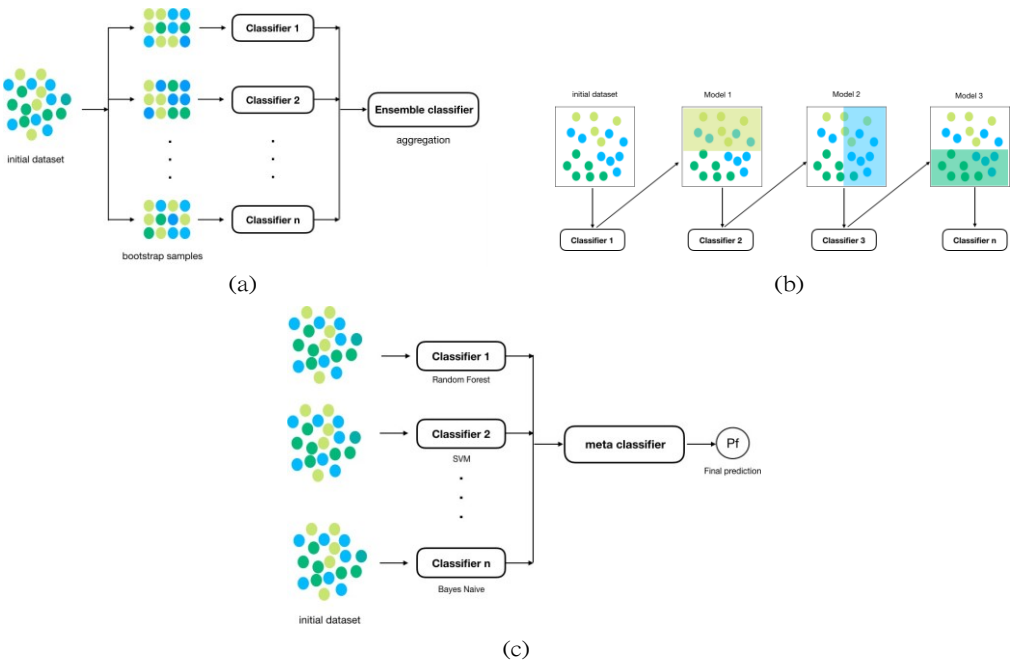

Figure 5. (a) Bagging (b) Boosting (c) Stacking

test set while the rest are used to train the model. This procedure is repeated until each fold of 4 folds has been used as a test set. The stratified k-fold is a variety of k-fold that initially shuffles the data set and split it into several folds to ensure that each fold is an appropriate representation of the whole data set as shown in Figure 6b. Figure 6c shows the Leave-one-out cross-validation (LOOCV) procedure. LOOCV separates one data point from the training data as test data and leaves the others as data to train the model. This is repeated for all combinations for the data provided. Therefore stratified-k fold technique was applied on our constrained data set to produce multiple data set in order to have preliminary indication the mechanism disruption of each exposed toxin. In addition, stratified k-fold CV was applied in this study because it produced best accuracy performance.

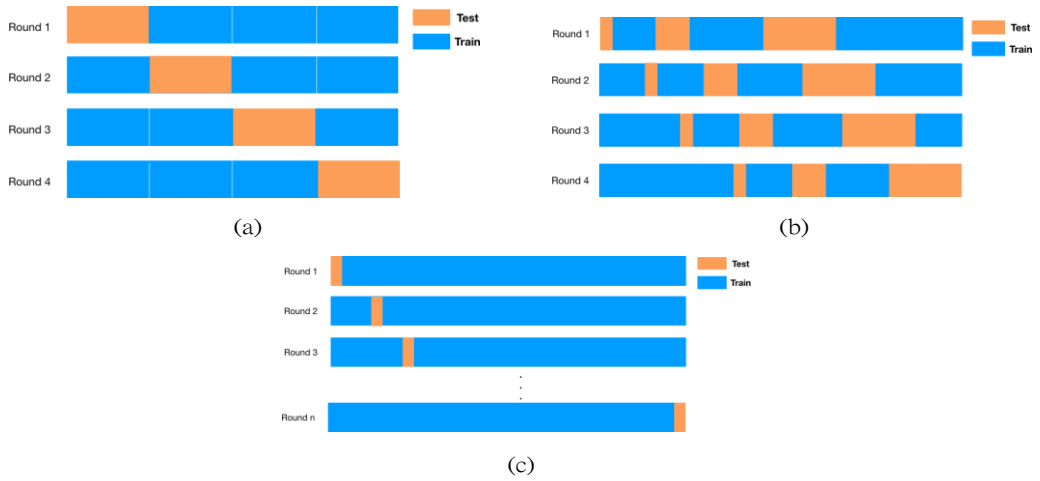

Figure 6. Type of cross-validation (a) k-fold (b) Stratified k-fold (c) LOOCV

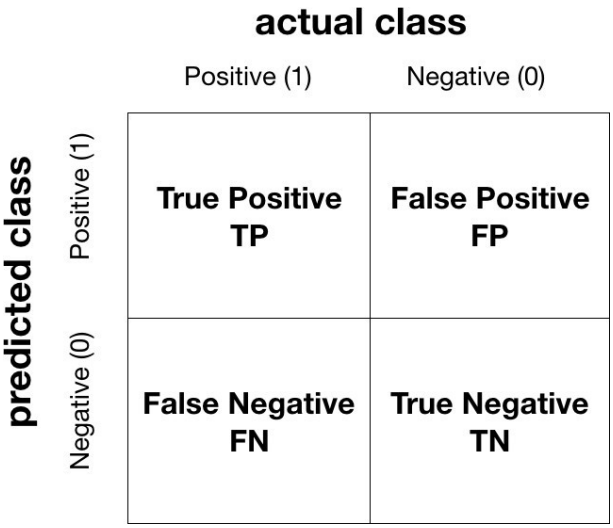

Figure 7. Confusion matrix of classification

2.4.2. *Confusion matrix*

Classification performance can be represented by a confusion matrix. A confusion matrix is the prediction table made by a classification model. The columns of the matrix are related to the actual of the data, and the rows of the matrix are related to the prediction by the model. Figure 7 shows confusion matrix for binary classifier which have four possible outcomes. True Positive (TP) is the condition when the prediction is positive and it's true. True Negative (TN) is the condition when the prediction is negative and it's true. False Positive (FP) is the condition when the prediction is positive and it's false. False Negative (FN) is the condition when the prediction is negative and it's false.

The performance of classification is defined in three categories. They are recall (R_c), precision (P_r), accuracy and it is defined as follows :

$$Rc = \frac{TP\ TP}{+\ FN} \tag{2}$$

$$Pr = \frac{TP}{TP + FP} \tag{3}$$

$$Accuracy = \frac{TP + TN}{TP + FP + FN + TN} \tag{4}$$

2.4.3. Receiver Operator Characteristic

Receiver Operator Characteristic (ROC) curve shows the plot between the True Positive Rate (TPR=TP/(TP+FN)) and the False Positive Rate (FPR=FP/(FP+TN)). Classifiers that provide curves that are closer to the top left corner indicate better performance. While classifiers that provide curves closer to the 45-degree diagonal line indicate less accurate model performance The curve shows the diagnostic ability of binary classifier for each class in data set. Area Under Curve (AUC) represents the ability of the model to separate each class. A good model has AUC value close to 1 and a poor model has a value close to 0. Macro averaging (Pr_{macro}) reduces multiclass predictions to a set of binary predictions by calculating average of entire precision (Pr) results. Micro averaging (Pr_{micro}) makes the all data set as an aggregate result by calculating all true positive results and divide it by sum of true positive results and false positive results and defined as follows:

$$Pr_{macro} = \frac{Pr_1 + Pr_2 + \ldots + Pr_k}{k} \tag{5}$$

$$Pr_{micro} = \frac{TP_1 + TP_2 + \ldots + TP_k}{(TP_1 + TP_2 + \ldots + TP_k) + (FP_1 + FP_2 + \ldots + FP_k)} \tag{6}$$

In this study, data were divided into two groups; training set (70%) and test set or predictor (30%) for each ensemble classification technique. The training set is used for making a classification model and test set is used for evaluating the performance of the classification model.

3. Results and analysis

Before the machine learning algorithm was applied to the data or measurement results, the data set was visualised using t-distributed Stochastic Neighbor Embedding (t-SNE) (van der Maaten and Hinton 2008). t-SNE is an algorithm to reduce the dimensionality of data. The algorithm projects multi-dimensional data into a 2D or 3D representation. t-SNE was chosen because it is able to ensure that adjacent points in the high dimension, tend to stay close together in the low dimension. Figure 8 shows the t-SNE plot consisting of 4 clusters namely control, H_2O_2, DMSO and Saponin. From

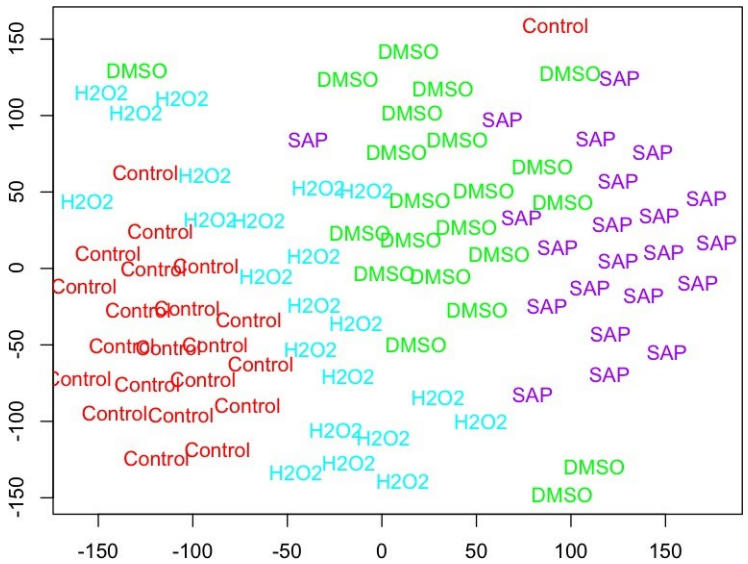

Figure 8. Visualisation the data set using t-SNE algorithm

the figure, the data for the each of the toxin and the control are clearly separated. However, there are a small number of outliers, which are significantly different from the main dataset, for each of the categories. This may relate to issues in the experiment or particular, complex responses of the cells. A number of data analysis techniques are available to remove outliers.

At the beginning, base learners were chosen based on inducing class to use different base level algorithms and one algorithm with various parameters and train each on the same data set but the accuracy results were still not as expected (smaller than 0.5), therefore the ensemble method was applied to improve the predictive performance by decrease variance (bagging), reduce bias (boosting) and improve predictions (stacking). Based on the the complementarity combinations of the base learners that have been tried, the combination that produces the highest accuracy was selected.

To build a predictive model of machine learning, the first method used was RF using the stratified k-fold CV method. In this study, the stratified 8-fold CV was used to estimate the RF model against measured data. Another tuning parameter used was *mtry* with values 2, 4, 8 and 15. This parameter indicates the number of variables sampled for splitting at each node. Figure 9 shows the accuracy of the model that was created. The accuracy of the model decreases relative to the predictor 3 and increases to the predictor 4.

The confusion matrix of RF using test data is depicted in Figure 10a. The accuracy of using test data was 0.625 and Root Mean Squared Error (RMSE) was 0.3819. Figure 10b shows the ROC of the model performance for all classes using RF. The figure also depicts the ROC curve plus the Area Under Curve (AUC) for each class. It revealed that performance of the model gave a relatively satisfactory result, demonstrated by the fact that the curve that is not close to the diagonal line and AUC values of each class are above 0.5.

By using *gbm*, the tuning parameters used are interaction depth, shrinkage and minobsinnode. The interaction depth is a parameter which indicates the number of splits that has to be conducted on a tree, which were 1,5 and 9 in this study. The

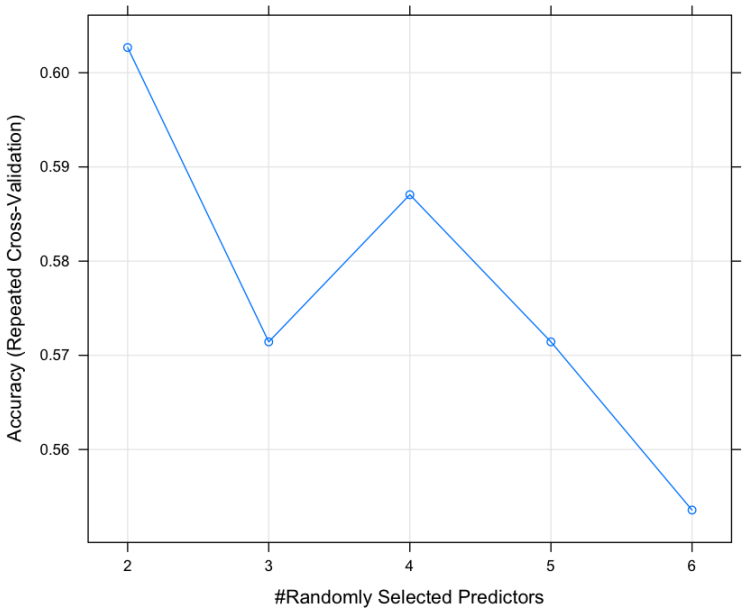

Figure 9. Model accuracy of RF using various iterations using stratified k-fold CV

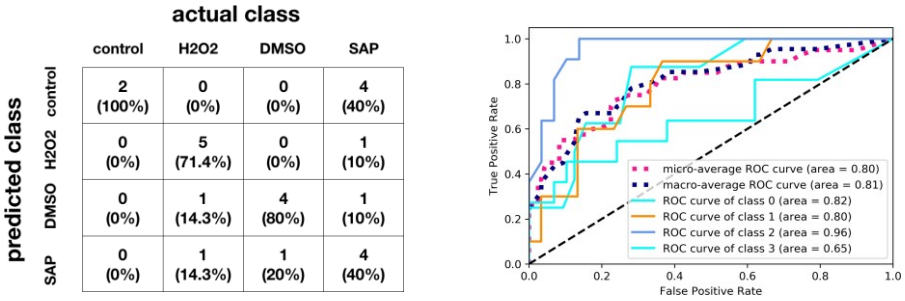

predicted class	actual class: control	H2O2	DMSO	SAP
control	2 (100%)	0 (0%)	0 (0%)	4 (40%)
H2O2	0 (0%)	5 (71.4%)	0 (0%)	1 (10%)
DMSO	0 (0%)	1 (14.3%)	4 (80%)	1 (10%)
SAP	0 (0%)	1 (14.3%)	1 (20%)	4 (40%)

(a) (b)

Figure 10. (a) The row is a prediction, while the actual column or class states the output of RF. (b) ROC of the classification using RF

minobsinnode is a parameter that tells every decision tree that is formed when to stop. The values of the tuning parameter used in this study were shrinkage 0.01, 0.05 and 0.1 and minobsinnode 3, 5 and 7. In addition, the stratified 8-fold CV was also applied as shown in Figure 11. The combination of these parameters produced best accuracy approximately 0.65 for minobsinnode 3, shringkage 0.01 and interaction depth 1.

Figure 12a shows a confusion matrix using test data which produces an accuracy of 0.625. In addition, Figure 12b shows plots for the ROC curves of the *gbm*. From the ROC curve it can be seen that all AUCs from all classes were above 0.5, which indicates that the model performance was relatively good.

Figure 13 shows the box plot of accuracy for various classifiers and stacking using the stratified 10-fold CV. The figure reveals that the average accuracy of stacking shows better results compared with the individual classifier used in stacking which was 0.615. Figure 14a shows the confusion matrix of stacking using test data set with accuracy 0.625. The ROC curve of the stacking model is shown in Figure 14b. All

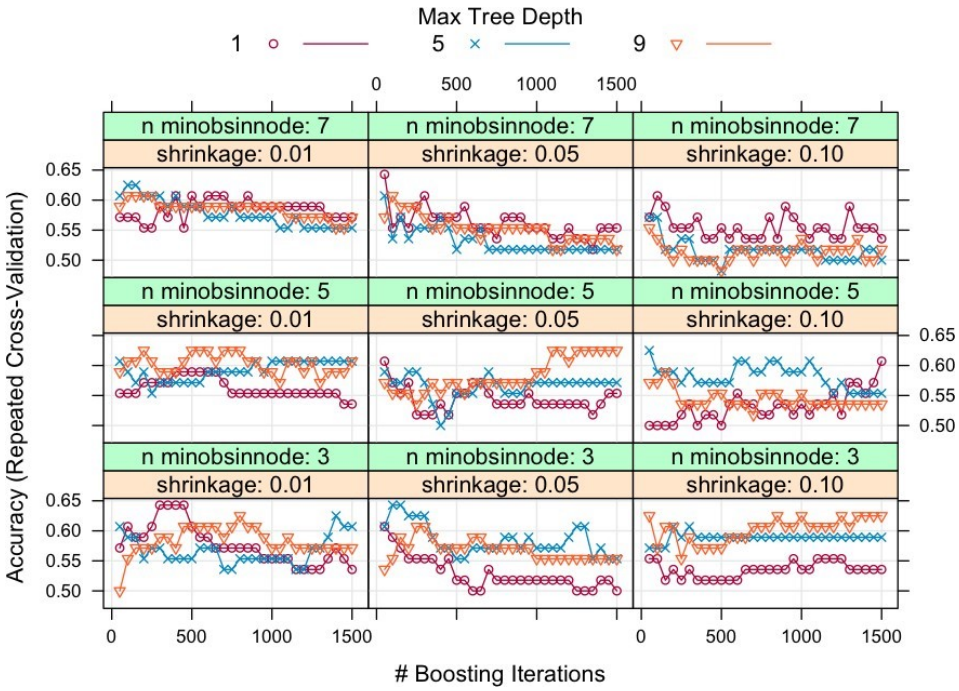

Figure 11. Model accuracy of gbm using different boosting iterations

curves are quite far from the diagonal line which shows a good performance, especially class 2. The AUC also show a relatively good values (particularly for class 2) showing the ability of the model to distinguish between classes.

In commercial toxicity testing and drug discovery vast numbers of materials are tested. The aim is to classify key biological indicators of materials–cell interaction with respect to material dose and time, allowing predication of in-vivo adverse effects. Traditionally, colorimetric or fluorometric endpoints are used to determine cytotoxic effects, but impedance based sensing methods have benefits that they are non-invasive and can be performed in real time (Gasser et al. 2020). To be appropriate for this application, the output from the impedance sensor system must classify toxins/materials according to particular molecular structures within the material or

predicted class \ actual class	control	H2O2	DMSO	SAP
control	3 (100%)	0 (0%)	0 (0%)	3 (37.5%)
H2O2	0 (0%)	5 (71.4%)	0 (0%)	1 (12.5%)
DMSO	0 (0%)	1 (14.3%)	4 (57%)	1 (12.5%)
SAP	0 (0%)	0 (14.3%)	3 (43%)	3 (37.5%)

(a)

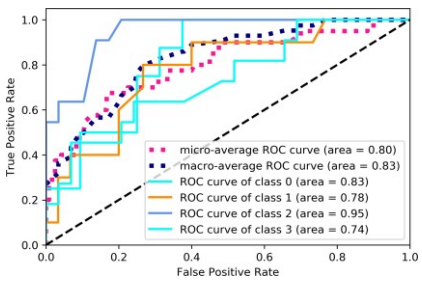

(b)

Figure 12. (a) The row is a prediction, while the actual column or class states the output of gbm. (b) ROC of the classification using gbm

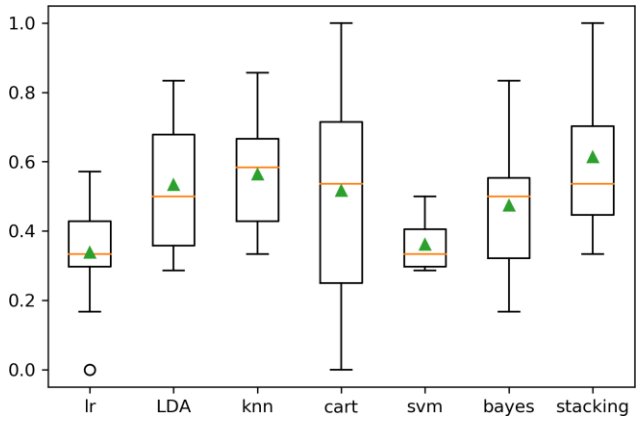

Figure 13. Model accuracy of stacking from various machine learning algorithms

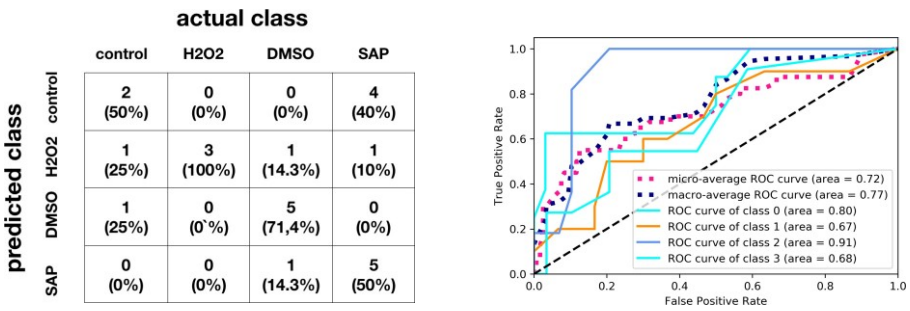

predicted class \ actual class	control	H2O2	DMSO	SAP
control	2 (50%)	0 (0%)	0 (0%)	4 (40%)
H2O2	1 (25%)	3 (100%)	1 (14.3%)	1 (10%)
DMSO	1 (25%)	0 (0`%)	5 (71,4%)	0 (0%)
SAP	0 (0%)	0 (0%)	1 (14.3%)	5 (50%)

(a) (b)

Figure 14. (a) The row is a prediction, while the actual column or class states the output of stacking (b) ROC of the classification using stacking

modes of action (in a similar way to the traditional techniques). Consequently, during toxicity testing or drug discovery the impedance response of a new material can be compared with a library of impedance data to identify the type of toxic effect (if any) the material exhibits. The work presented in this paper presents a new technique that potentially could be used to create the library and assess materials relative to this. In order to create a comprehensive library suitable to be used for toxicity testing and drug discovery, tests, subsequent feature extraction and machine learning, would need to be performed on a broad range of cell lines using many toxins. Future work is involving expanding the range of toxins including the evaluation of those with very specific modes of action on the cell.

4. Conclusions

Cytotoxicity tests have been carried out on EC304 cells using 3 types of toxins namely H_2O_2, DMSO and Saponin, using impedance spectroscopy. The impedance data from these tests produce a number of features extracted using the Detrended Fluctuation Analysis (DFA) method. These features were used as training data for machine learning with ensemble techniques. Random Forest (RF), gradient boosting machine (gbm) and stacking algorithms were used to classify the results from the 3 types of toxin applied to ECV304 cells. Data processing using the ensemble classification demonstrated that the algorithm *gbm* method provided better performance of model results compared to RF and stacking in terms of accuracy. These results indicated that impedance spectroscopy results from cytotoxicity tests can be classified based on the type of toxin applied to the cells. This shows that the feature extraction methodologies performed could distinguish morphological changes, which caused differences in impedance spectra of the cell culture depending on the type of toxin applied.

References

Aliyu HA, Sudirman R, Razak MAA, Wahab MAA. 2018. Red Blood Cell Classification: Deep Learning Architecture Versus Support Vector Machine. In: 2018 2nd International Conference on BioSignal Analysis, Processing and Systems (ICBAPS); Jul. p. 142–147.

Arndt S, Seebach J, Psathaki K, Galla HJ, Wegener J. 2004. Bioelectrical impedance assay to monitor changes in cell shape during apoptosis. Biosensors and Bioelectronics. 19(6):583–594. [accessed 2020-08-13]. Available from: http://www.sciencedirect.com/science/article/pii/S0956566303002690.

Barsoukov E, Macdonald JR. 2005. Impedance Spectroscopy: Theory, Experiment, and Applications. John Wiley & Sons. Google-Books-ID: 8hNkOWO_DLwC.

Bishop C. 2006. Pattern Recognition and Machine Learning. New York: Springer-Verlag. Information Science and Statistics; [accessed 2020-05-26]. Available from: https://www.springer.com/gp/book/9780387310732.

Breiman L. 1996. Bagging Predictors. Machine Learning. 24(2):123–140. [accessed 2020-05-21]. Available from: https://doi.org/10.1023/A:1018054314350.

Ceriotti L, Ponti J, Broggi F, Kob A, Drechsler S, Thedinga E, Colpo P, Sabbioni E, Ehret R, Rossi F. 2007. Real-time assessment of cytotoxicity by impedance measurement on a 96-well plate. Sensors and Actuators B: Chemical. 123(2):769–778. [accessed 2020-08-13]. Available from: http://www.sciencedirect.com/science/article/pii/S0925400506007015.

Chen T, Chefd'hotel C. 2014. Deep Learning Based Automatic Immune Cell Detection for Immunohistochemistry Images. In: Wu G, Zhang D, Zhou L, editors. Machine Learning in

Medical Imaging. Springer International Publishing. p. 17–24. Lecture Notes in Computer Science.
Cong J, Wei B, He Y, Yin Y, Zheng Y. 2017. A Selective Ensemble Classification Method Combining Mammography Images with Ultrasound Images for Breast Cancer Diagnosis. [accessed 2019-05-19]. Available from: https://www.hindawi.com/journals/cmmm/2017/4896386/.
Djawad YA, Attwood D, Kiely J, Luxton R. 2019. The application of detrended fluctuation analysis to assess physical characteristics of the human cell line ECV304 following toxic challenges. Sensing and Bio-Sensing Research. 23:100269. [accessed 2020-03-17]. Available from: http://www.sciencedirect.com/science/article/pii/S2214180418301260.
Ekins S, Puhl AC, Zorn KM, Lane TR, Russo DP, Klein JJ, Hickey AJ, Clark AM. 2019. Exploiting machine learning for end-to-end drug discovery and development. Nature Materials. 18(5):435. [accessed 2019-07-18]. Available from: https://www.nature.com/articles/s41563-019-0338-z.
Forslöw A. 2018. An investigation of Recent Deep Learning Techniques Applied to Blood Cell Image Analysis. Master's Theses in Mathematical Sciences. [accessed 2019-07-16]. Available from: http://lup.lub.lu.se/student-papers/record/8957638.
Gasser A, Eveness J, Kiely J, Attwood D, Luxton R. 2020. A non-contact impedimetric biosensing system for classification of toxins associated with cytotoxicity testing. Bioelectrochemistry. 133:107448. [accessed 2020-08-15]. Available from: http://www.sciencedirect.com/science/article/pii/S1567539419306619.
Gu Y, Zhang AC, Han Y, Li J, Chen C, Lo YH. 2019. Machine Learning Based Real-Time Image-Guided Cell Sorting and Classification. Cytometry Part A. 95(5):499–509. [accessed 2019-07-16]. Available from: https://onlinelibrary.wiley.com/doi/abs/10.1002/cyto.a.23764.
Hijazi H, Chan C. 2013. A Classification Framework Applied to Cancer Gene Expression Profiles. Journal of healthcare engineering. 4(2). [accessed 2019-05-19]. Available from: https://www.ncbi.nlm.nih.gov/pmc/articles/PMC3873740/.
Hijazi H, Wu M, Nath A, Chan C. 2012. Ensemble Classification of Cancer Types and Biomarker Identification. Drug development research. 73(7):414–419. [accessed 2019-05-19]. Available from: https://www.ncbi.nlm.nih.gov/pmc/articles/PMC4162531/.
Iqbal MS, El-Ashram S, Hussain S, Khan T, Huang S, Mehmood R, Luo B. 2019. Efficient cell classification of mitochondrial images by using deep learning. Journal of Optics. 48(1):113–122. [accessed 2019-07-16]. Available from: https://doi.org/10.1007/s12596-018-0508-4.
Kihm A, Kaestner L, Wagner C, Quint S. 2018. Classification of red blood cell shapes in flow using outlier tolerant machine learning. PLoS Computational Biology. 14(6). [accessed 2019-07-19]. Available from: https://www.ncbi.nlm.nih.gov/pmc/articles/PMC6021115/.
Lam VK, Nguyen T, Phan T, Chung BM, Nehmetallah G, Raub CB. 2019. Machine learning and phase signatures in cell line classification. In: Digital Holography and Three-Dimensional Imaging 2019 (2019), paper Th4A.2; May. Optical Society of America. p. Th4A.2. [accessed 2019-07-16]. Available from: https://www.osapublishing.org/abstract.cfm?uri=DH-2019-Th4A.2.
Liu R, Zhang G, Yang Z. 2019. Towards rapid prediction of drug-resistant cancer cell phenotypes: single cell mass spectrometry combined with machine learning. Chemical Communications. 55(5):616–619. [accessed 2019-07-17]. Available from: https://pubs.rsc.org/en/content/articlelanding/2019/cc/c8cc08296k.
Meng N, Lam E, Tsia KKM, So HKH. 2018. Large-scale Multi-class Image-based Cell Classification with Deep Learning. IEEE journal of biomedical and health informatics.
Nassar M, Doan M, Filby A, Wolkenhauer O, Fogg DK, Piasecka J, Thornton CA, Carpenter AE, Summers HD, Rees P, et al. 2019. Label-Free Identification of White Blood Cells Using Machine Learning. Cytometry Part A. 0(0). [accessed 2019-07-19]. Available from: https://onlinelibrary.wiley.com/doi/full/10.1002/cyto.a.23794.
Oei RW, Hou G, Liu F, Zhong J, Zhang J, An Z, Xu L, Yang Y. 2019. Convolutional neural network for cell classification using microscope images of intracellular actin networks. PLOS ONE. 14(3):e0213626. [accessed 2019-07-15]. Available from:

https://journals.plos.org/plosone/article?id=10.1371/journal.pone.0213626.
Ozaki Y, Yamada H, Kikuchi H, Hirotsu A, Murakami T, Matsumoto T, Kawabata T, Hiramatsu Y, Kamiya K, Yamauchi T, et al. 2019. Label-free classification of cells based on supervised machine learning of subcellular structures. PLOS ONE. 14(1):e0211347. [accessed 2019-07-17]. Available from: https://journals.plos.org/plosone/article?id=10.1371/journal.pone.0211347.
Pan WD, Dong Y, Wu D. 2018. Classification of Malaria-Infected Cells Using Deep Convolutional Neural Networks. Machine Learning - Advanced Techniques and Emerging Applications.
Park C, Cho SB. 2003. Evolutionary Computation for Optimal Ensemble Classifier in Lymphoma Cancer Classification. In: Zhong N, Raś ZW, Tsumoto S, Suzuki E, editors. Foundations of Intelligent Systems. Springer Berlin Heidelberg. p. 521–530. Lecture Notes in Computer Science.
Peng C, Havlin S, Stanley H, Goldberger A. 1995. Quantification of scaling exponent and crossover phenomena in nonstationary heart beat time series. Chaos. 5:82–87.
Rachman AA, Rustam Z. 2016. Cancer classification using Fuzzy C-Means with feature selection. In: 2016 12th International Conference on Mathematics, Statistics, and Their Applications (ICMSA); Oct. p. 31–34.
Ren D, Chui CO. 2018. Feasibility of Tracking Multiple Single-Cell Properties with Impedance Spectroscopy. ACS Sensors. 3(5):1005–1015. Publisher: American Chemical Society; [accessed 2020-08-13]. Available from: https://doi.org/10.1021/acssensors.8b00152.
Rubin M, Stein O, Turko NA, Nygate Y, Roitshtain D, Karako L, Barnea I, Giryes R, Shaked NT. 2019. TOP-GAN: Label-free cancer cell classification using deep learning with a small training set. Medical Image Analysis. [accessed 2019-07-16]. Available from: http://www.sciencedirect.com/science/article/pii/S1361841519300568.
Schapire RE. 1990. The strength of weak learnability. Machine Learning. 5(2):197–227. [accessed 2020-05-21]. Available from: https://doi.org/10.1007/BF00116037.
Sengupta SK, Farnham JM, Whitten JE. 2005. A Simple Low-Cost Lock-In Amplifier for the Laboratory. Journal of Chemical Education. 82(9):1399. Publisher: American Chemical Society; [accessed 2020-03-27]. Available from: https://doi.org/10.1021/ed082p1399.
Singh SP, Janjuha S, Chaudhuri S, Reinhardt S, Dietz S, Eugster A, Bilgin H, Korkmaz S, Reid JE, Zararsiz G, et al. 2018. Machine learning based classification of cells into chronological stages using single-cell transcriptomics. bioRxiv:303214. [accessed 2019-07-16]. Available from: https://www.biorxiv.org/content/10.1101/303214v1.
Sommer C, Gerlich DW. 2013. Machine learning in cell biology – teaching computers to recognize phenotypes. Journal of Cell Science. 126(24):5529–5539. [accessed 2019-07-16]. Available from: https://jcs.biologists.org/content/126/24/5529.
Suda K, Rothen-Rutishauser B, Günthert M, Wunderli-Allenspach H. 2001. Phenotypic characterization of human umbilical vein endothelial (ECV304) and urinary carcinoma (T24) cells: Endothelial versus epithelial features. In Vitro Cellular & Developmental Biology - Animal. 37(8):505–514. [accessed 2020-08-13]. Available from: https://doi.org/10.1290/1071-2690(2001)037i0505:PCOHUV¿2.0.CO;2.
Tarek S, Elwahab RA, Shoman M. 2016. Cancer classification ensemble system based on gene expression profiles. In: 2016 5th International Conference on Electronic Devices, Systems and Applications (ICEDSA); Dec. p. 1–4.
Tiwari P, Qian J, Li Q, Wang B, Gupta D, Khanna A, Rodrigues JJPC, de Albuquerque VHC. 2018. Detection of subtype blood cells using deep learning. Cognitive Systems Research. 52:1036–1044. [accessed 2019-07-19]. Available from: http://www.sciencedirect.com/science/article/pii/S1389041718303760.
van der Maaten L, Hinton G. 2008. Visualizing data using t-SNE. Journal of Machine Learning Research. 9:2579–2605. Available from: http://www.jmlr.org/papers/v9/vandermaaten08a.html.
Vlahou A, Schorge JO, Gregory BW, Coleman RL. 2003. Diagnosis of Ovarian Cancer Using Decision Tree Classification of Mass Spectral Data. Journal of

Biomedicine and Biotechnology. 2003(5):308–314. [accessed 2019-05-18]. Available from: https://www.ncbi.nlm.nih.gov/pmc/articles/PMC521504/.
Wang CW. 2006. New Ensemble Machine Learning Method for Classification and Prediction on Gene Expression Data. In: 2006 International Conference of the IEEE Engineering in Medicine and Biology Society; Aug. p. 3478–3481.
Wang L, Wang L, Yin H, Xing W, Yu Z, Guo M, Cheng J. 2010. Real-time, label-free monitoring of the cell cycle with a cellular impedance sensing chip. Biosensors & Bioelectronics. 25(5):990–995.
William W, Ware A, Basaza-Ejiri AH, Obungoloch J. 2019. Cervical cancer classification from Pap-smears using an enhanced fuzzy C-means algorithm. Informatics in Medicine Unlocked. 14:23–33. [accessed 2019-05-19]. Available from: http://www.sciencedirect.com/science/article/pii/S2352914818302478.
Wolpert DH. 1992. Stacked generalization. Neural Networks. 5(2):241–259. [accessed 2020-05-21]. Available from: http://www.sciencedirect.com/science/article/pii/S0893608005800231.
Xia F, Shukla M, Brettin T, Garcia-Cardona C, Cohn J, Allen JE, Maslov S, Holbeck SL, Doroshow JH, Evrard YA, et al. 2018. Predicting tumor cell line response to drug pairs with deep learning. BMC Bioinformatics. 19(18):486. [accessed 2019-07-17]. Available from: https://doi.org/10.1186/s12859-018-2509-3.
Yang JH, Wright SN, Hamblin M, McCloskey D, Alcantar MA, Schrübbers L, Lopatkin AJ, Satish S, Nili A, Palsson BO, et al. 2019. A White-Box Machine Learning Approach for Revealing Antibiotic Mechanisms of Action. Cell. 177(6):1649–1661.e9. [accessed 2019-07-17]. Available from: https://www.cell.com/cell/abstract/S0092-8674(19)30402-7.
Yin Z, Ai H, Zhang L, Ren G, Wang Y, Zhao Q, Liu H. 2019. Predicting the cytotoxicity of chemicals using ensemble learning methods and molecular fingerprints. Journal of applied toxicology: JAT.
Zhao R, Gu L, Zhu X. 2019. Combining Fuzzy C-Means Clustering with Fuzzy Rough Feature Selection. Applied Sciences. 9(4):679. [accessed 2019-05-19]. Available from: https://www.mdpi.com/2076-3417/9/4/679.
Zitnik M, Nguyen F, Wang B, Leskovec J, Goldenberg A, Hoffman MM. 2019. Machine learning for integrating data in biology and medicine: Principles, practice, and opportunities. Information Fusion. 50:71–91. [accessed 2020-03-25]. Available from: http://www.sciencedirect.com/science/article/pii/S1566253518304482.